Int. J. of Applied Mechanics and Engineering, 2020, vol.25, No.1, pp.92-105
DOI: 10.2478/ijame-2020-0007

A NON-SINGULAR ANALYTICAL TECHNIQUE FOR REINFORCED NON-CIRCULAR HOLES IN ORTHOTROPIC LAMINATE

PRADEEP MOHAN
Mar Baselios College of Engineering and Technology
Thiruvananthapuram - 695015, INDIA

R. RAMESH KUMAR*
Department of Mechanical Engineering
Sree Chitra Thirunal College of Engineering
Thiruvananthapuram - 695035, INDIA
E-mail: rameshkumar9446@gmail.com

The intricacy in Lekhnitskii's available single power series solution for stress distribution around hole edge for both circular and noncircular holes represented by a hole shape parameter ε is decoupled by introducing a new technique. Unknown coefficients in the power series in ε are solved by an iterative technique. Full field stress distribution is obtained by following an available method on Fourier solution. The present analytical solution for reinforced square hole in an orthotropic infinite plate is derived by completely eliminating stress singularity that depends on the concept of stress ratio. The region of validity of the present analytical solution on reinforcement area is arrived at based on a comparison with the finite element analysis. The present study will also be useful for deriving analytical solution for orthotropic shell with reinforced noncircular holes.

Key words: power series, stress ratio, non-circular hole.

1. Introduction

Composite structures invariably have reinforced holes in aerospace industries. Holes are also reinforced during repair. Lekhnitskii [1] obtained the distribution of stresses around unreinforced holes in an orthotropic plate for different shape parameter, ε which represents noncircular holes. Following Lekhnitskii [1], Rajaiah and Naik [2] obtained stress distribution for a square hole with ε = *-1/9* having a corner radius of *0.2* times hole width in an infinite orthotropic plate and perturbed ε to arrive at an optimum hole in the form of a double barrel shape that has uniform stress distribution in tension and compression regions (Appendix A). It is well known that due to micro mechanical behavior at the hole edge, strength of the laminate is much higher than theoretical prediction. This concept was experimentally proved by Whitney and Nuismer [3], and evolved point stress criterion that requires stress distribution ahead of a circular hole. This was analytically derived by Konish and Whitney [4]. However, for a highly orthotropic laminate (E_L/E_T=55) their solution becomes invalid. For such cases, Kumar *et al.* [5], following an inverse approach based on Lekhnitskii's solution, obtained an expected result ahead of the hole by considering the Fourier series approach.

In the present work, Lekhnitskii's solution for a non-circular hole in terms of ε, is suitably manipulated and expressed in unknown Fourier coefficients for obtaining full field stress distribution and is extended for reinforced square holes. An iterative procedure is followed to determine the unknown coefficients. A uniform reinforcement region over the plate surface around a square or noncircular hole (defined by ε) obtained by the present analytical expression is confirmed by the finite element analysis.

* To whom correspondence should be addressed

2. Method of approach

The available Lekhnitskii's solution for tangential stress distribution around a non-circular hole edge in an infinite laminate plate under uniaxial tension is given in terms of ε as

$$\sigma_\theta = p\frac{B^2}{C^2} + \frac{p}{LC^2}\left\{\begin{array}{l} AD^4\cos\theta + BC^4 n\sin\theta - \varepsilon\Big[AC^4 dkn\cos\theta + 3AD^4\cos 3\theta + \\ +BC^4\left(l\sin\theta + 3\sin 3\theta\right)\Big] - \varepsilon^2 C^4 n\Big(Ak\Big(r\cos AC^4 dkn\cos\theta + 3AD^4\cos 3\theta + \\ BC^4\left(l\sin\theta + 3h\sin 3\theta\right)\Big)\Big) \end{array}\right\}. \tag{2.1}$$

The contour of square holes and noncircular holes corresponding to ε is given in Appendix A.
The terms in Eq.(2.1) are depicted in Appendix B.

2.1. σ_θ/ σ as a sum of each individual term in ε

In the present study, Lekhnitskii's solution is expressed in separate trigonometric series with orthotropic constants corresponding to each order in ε. As constants A and B are given in terms of ε, σ_θ /σ is expressed in the full power series of ε up to ε^7 by substituting A, B, C, D and L in Eq.(2.1) as

$$\frac{\sigma_\theta}{\sigma} = \frac{x_0 + \varepsilon x_1 + \varepsilon^2 x_2 + \varepsilon^3 x_3 + \varepsilon^4 x_4 + \varepsilon^5 x_5 + \varepsilon^6 x_6 + \varepsilon^7 x_7}{X_0 + \varepsilon X_1 + \varepsilon^2 X_2 + \varepsilon^3 X_3 + \varepsilon^4 X_4 + \varepsilon^5 X_5 + \varepsilon^6 X_6 + \varepsilon^7 X_7} \tag{2.2}$$

where, x_0, x_1, x_2….and X_0, X_1, X_2... are cosine series with cosine terms up to cos18θ.
For terms independent of ε, x_0 is given by

$$\begin{aligned} x_0 &= x_{00} + x_{02}\cos 2\theta + x_{04}\cos 4\theta + x_{06}\cos 6\theta + x_{08}\cos 8\theta + x_{010}\cos 10\theta + \\ &+ x_{012}\cos 12\theta + x_{014}\cos 14\theta + x_{016}\cos 16\theta + x_{018}\cos 18\theta \end{aligned} \tag{2.3}$$

and x_i as

$$\begin{aligned} x_i &= x_{i0} + x_{i2}\cos 2\theta + x_{i4}\cos 4\theta + x_{i6}\cos 6\theta + x_{i8}\cos 8\theta + x_{i10}\cos 10\theta + \\ &+ x_{i12}\cos 12\theta + x_{i14}\cos 14\theta + x_{i16}\cos 16\theta + x_{i18}\cos 18\theta \end{aligned} \tag{2.4}$$

for $i = 1, 2, 3, 4, 5, 6$ and 7.
In a similar way for terms in the denominator X_0 and X_i in Eq.(2.2) can be represented by replacing x by X in Eq.(2.3) and Eq.(2.4).
In other words, σ_θ /σ can be expressed as

$$\sigma_\theta/\sigma = \frac{\sum_{i=0}^{\infty} x_i \varepsilon^i}{\sum_{i=0}^{\infty} X_i \varepsilon^i}. \tag{2.5}$$

It is possible to obtain σ_θ/σ as a target expression of $\sum_{i=0}^{\infty} c_i \varepsilon^i$ as described in Appendix C. Applying the standard iterative method, the coefficient of ε, c_i can be determined using the following equation.

$$\text{For} \qquad i>0, \quad c_i = \frac{x_i - \sum_{j=0}^{i-1} c_j X_{i-j}}{X_o}, \tag{2.6}$$

c_i can be expressed as n_i/N_0. Thus σ_θ/σ can be written as

$$\frac{\sigma_\theta}{\sigma} = \frac{n_0}{N_0} + \varepsilon\left(\frac{n_1}{N_0}\right) + \varepsilon^2\left(\frac{n_2}{N_0}\right) + \ldots\ldots + \varepsilon^i\left(\frac{n_i}{N_0}\right). \tag{2.7}$$

The term n_0/N_0 which is independent of ε corresponds to the stress distribution around a circular hole in an orthotropic plate as Kumar *et al*. [5-6]

$$\frac{n_0}{N_0} = \frac{1-\cos 2\theta}{2} + \frac{1}{2\rho^2} - \frac{3}{2\rho^4}\cos 2\theta + \sum_{j=2}^{\infty} \frac{C_{2j}}{2}\left[\frac{4j-3}{\rho^{4j-2}} - \frac{4j-1}{\rho^{4j}}\right]\cos 2j\theta, \tag{2.8}$$

{isotropic plate solution} + {additional terms in ρ for orthotropic plate}
(circular hole) (circular hole)

ρ is the ratio of the distance of a point on the surface from the center of the hole, to the width or radius of the hole along the *x*-axis or *y*-axis.

2.2. Fourier terms

The first term in power series in ε is expressed as

$$c_1 = n_1/N_0 = (x_1 - N_1\, n_0/N_0)/N_0.$$

The above expression, being a division of two cosines series, can be written in a Fourier expression as given below.

$$\frac{S_0}{2} + \sum_{j=1}^{\infty} S_{2j}\cos 2j\theta. \tag{2.9}$$

The values of S_{2j} can be found out by using the standard technique for finding the Fourier coefficients by iteration as obtained by Krylov [7]. The methodology adopted is given in Appendix D.

In a similar way, each term n_i/N_0 for each power series in ε can be determined. The full field stress distribution in an isotropic plate with a square hole can be determined with the inclusion of parameter ρ along with the Fourier coefficients in the analytical expression. Using the methodology illustrated in Appendix D, the Fourier coefficients and the higher order terms in ρ can been found out and an additional term corresponding to stress distribution in an isotropic plate is expressed as

$$\sum_{i=1}^{\infty}\left[\varepsilon^{i}\sum_{j=1}^{\infty}\frac{Si_{2j}}{2}\left[\frac{4j-3}{\rho^{4j-2}}-\frac{4j-1}{\rho^{4j}}\right]\cos 2j\theta\right] \tag{2.10}$$

where S_i are the isotropic coefficients for a square hole with a rounded corner.

Stress distribution in an orthotropic plate can be written as a sum of stress distribution in an isotropic plate and additional terms due to the orthotropic property. Additional terms found out using the same sequence of analytical steps as illustrated in Appendix D, is given below.

$$\sum_{i=1}^{\infty}\left[\varepsilon^{i}\left(\sum_{j=0}^{1}\frac{(So\text{ - }Si)_{2j}}{4j\text{ - }2}\left(\frac{4j+1}{\rho^{4j+2}}-\frac{4j+3}{\rho^{4j+4}}\right)\cos 2j\theta+\sum_{j=2}^{\infty}\frac{(So\text{ - }Si)_{2j}}{2}\left(\frac{4j-3}{\rho^{4j-2}}-\frac{4j-1}{\rho^{4j}}\right)\cos 2j\theta\right)\right]. \tag{2.11}$$

The full field stress distribution in an orthotropic plate with a square hole can be written as the sum of stress distribution in an orthotropic plate with a circular hole and higher order terms of ρ and ε corresponding to isotropic and orthotropic material properties as given below

$$\left(\frac{\sigma_\theta}{\sigma}\right)_{ur}=\frac{1-\cos 2\theta}{2}+\frac{1}{2\rho^{2}}-\frac{3}{2\rho^{4}}\cos 2\theta \longrightarrow$$

isotropic plate solution (circular hole)

$$+$$

$$\sum_{j=2}^{\infty}\frac{C_{2j}}{2}\left[\frac{4j-3}{\rho^{4j-2}}-\frac{4j-1}{\rho^{4j}}\right]\cos 2j\theta \longrightarrow$$

additional terms in ρ for orthotropic plate (circular hole)

$$+$$

$$\sum_{i=1}^{\infty}\left[\varepsilon^{i}\sum_{j=1}^{\text{¥}}\frac{Si_{2j}}{2}\left[\frac{4j\text{ - }3}{\rho^{4j\text{-}2}}\text{ - }\frac{4j\text{ - }1}{\rho^{4j}}\right]\cos 2j\theta\right] \longrightarrow \tag{2.1}$$

additional term in isotropic plate (noncircular hole)

$$+$$

$$\sum_{i=1}^{\infty}\left[\varepsilon^{i}\left(\begin{array}{l}\displaystyle\sum_{j=0}^{1}\frac{(So\text{ - }Si)_{2j}}{4j\text{ - }2}\left(\frac{4j+1}{\rho^{4j+2}}-\frac{4j+3}{\rho^{4j+4}}\right)\cos 2j\theta+\\ \displaystyle+\sum_{j=2}^{\infty}\frac{(So\text{ - }Si)_{2j}}{2}\left(\frac{4j-3}{\rho^{4j-2}}-\frac{4j-1}{\rho^{4j}}\right)\cos 2j\theta\end{array}\right)\right] \longrightarrow$$

additional terms in ρ for orthotropic plate (noncircular hole)

where, *Ss* are the orthotropic coefficients for a square or a noncircular hole.

2.3.Stress ratio

The ratio of total thickness of the plate (in a closed region around the hole) including reinforcement thickness to virgin plate thickness is defined by the stress ratio. This ratio is derived from the ratio of σ_θ/σ of an unreinforced hole solution to that of reinforced hole.

$$\text{Stress ratio}=\frac{t+t_r}{t}=\frac{(\sigma_\theta/\sigma)_{ure}}{(\sigma_\theta/\sigma)_{re}}. \tag{2.13}$$

2.4. Tangential stress distribution around reinforced square hole (Appendix A)

It has been reported in Mohan and Kumar [8] that once an analytical solution for stress distribution of an unreinforced circular hole in a structure under a given loading is available, then it is possible to obtain in general, any target value for σ_θ/σ for a reinforced hole by simply considering the stress ratio, and even to arrive at a nonsingular solution! Thus Eq.(2.13) can be written as

$$\left(\frac{\sigma_\theta}{\sigma}\right)_{re}=\frac{t}{t+t_r}\left(\frac{\sigma_\theta}{\sigma}\right)_{ure}. \tag{2.14}$$

2.5. Finite element analysis

Finite element analysis is basically carried out to arrive at reinforcement area over the shell surface around the hole for a given target stress ratio of say, 2, so that Eq.(2.14) converges to the numerical result. It may be noted that for this stress ratio, the reinforcement thickness t_r equals the virgin plate thickness t (Fig.1., Eq.(2.13)). The uniform reinforcement scheme is followed to cater unforeseen design loads and also for easy fabrication process. It may be noted that the reinforcement thickness above and below the surface around the hole is taken as shown in Fig.1.

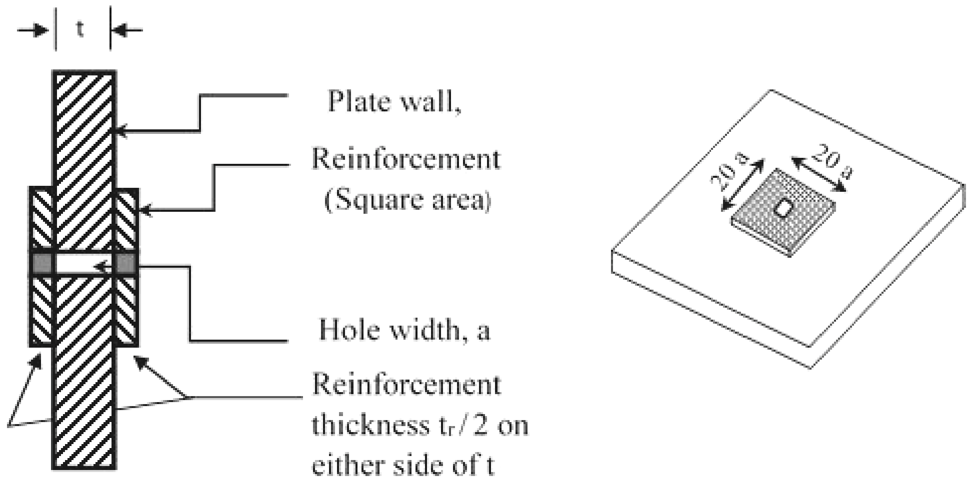

Fig.1. Reinforcement scheme.

A quarter portion of a plate containing a hole is modeled with a symmetric boundary condition along the symmetric planes as shown in Fig.2 with a four node shell element. A tensile load is applied appropriately. Material properties and dimensions of the plate for the current study are given in Tab.1. Initially, membrane stress distribution around the square hole in an orthotropic plate under uniaxial loading is obtained by the finite element analysis for unreinforced holes. Two analyses are carried out by progressively increasing reinforcement area over the plate surface around the hole till a good agreement for full filed stress distribution based on the present analytical solution is achieved.

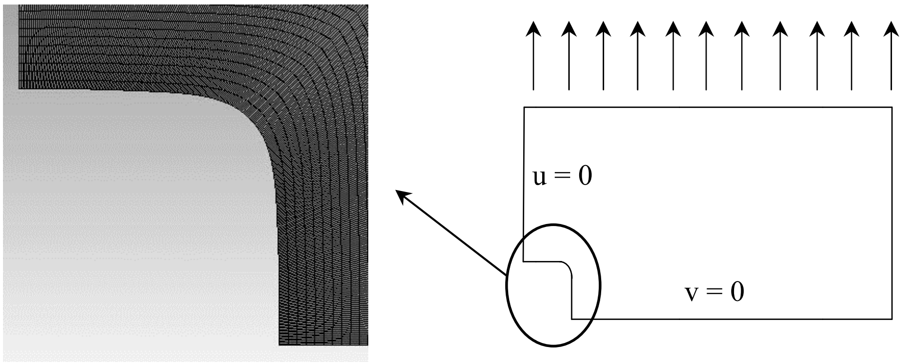

Fig.2. Finite Element Model of the plate.

Table 1. Material property.

E_L (GPa)	E_T (GPa)	G_{LT} (GPa)	υ_{LT}	Plate Thickness (*mm*)
329.5	*5.955*	*4.414*	*0.346*	*1.2*

3. Results and discussion

The present derivation for an unreinforced hole Eq.(2.12) based on Lekhnitskii's solution Eq.(2.1) is validated by comparing the results and given in Fig.3. For a constant reinforcement thickness corresponding to a stress ratio of 2, the area of reinforcement (Fig.1) around the hole is progressively increased symmetrically with respect to the hole to observe the convergence on variation of σ_θ/σ as given in Fig.4 for the unidirectional laminate. The comparison of analytical prediction with numerical results on the tangential stress distribution in an infinite orthotropic plate with an unreinforced and reinforced hole for layup sequence $(0)_{12}$, $(\pm 45_6)_S$, $(90)_{12}$ and $(0_4 \pm 45)_S$ with numerical result for stresses around the hole edge is shown in Fig.5. A comparison of full field stress distribution for the theoretical case in $(0)_{12}$ and $(\pm 45_6)_S$ plate with the finite element approach is depicted in Fig.6 and Fig.7. The present analytical prediction for reinforced hole is used to eliminate stress singularity that exists in the case of a highly orthotropic unidirectional laminate and shown in Fig.8.

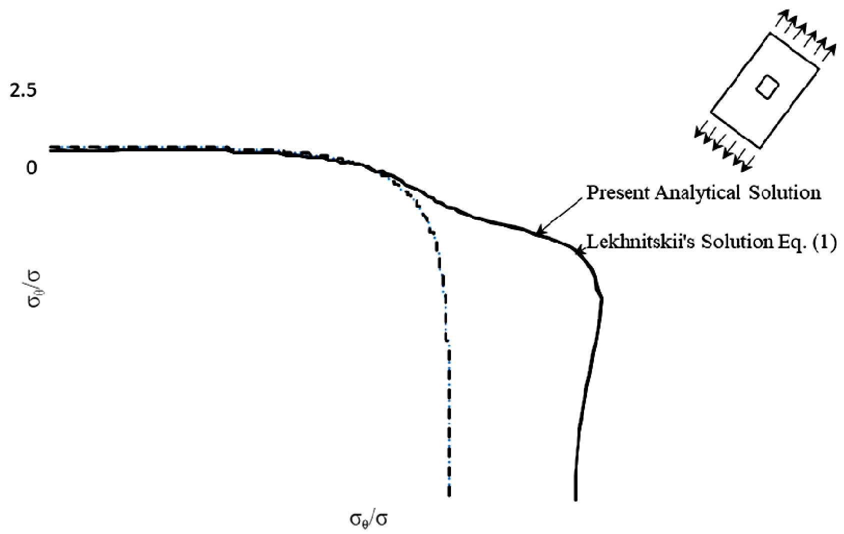

Fig.3. Comparison of stress distribution along the hole edge obtained by the present analytical solution andLekhnitskii's solution.

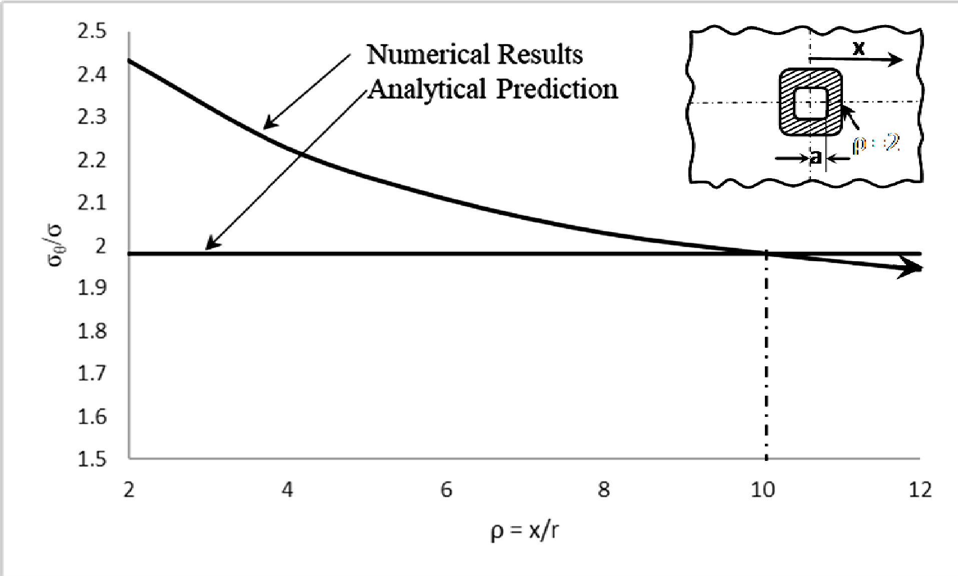

Fig.4. Comparison of maximum SCF along a reinforced square hole edge for various area of reinforcement obtained from analytical and numerical model.

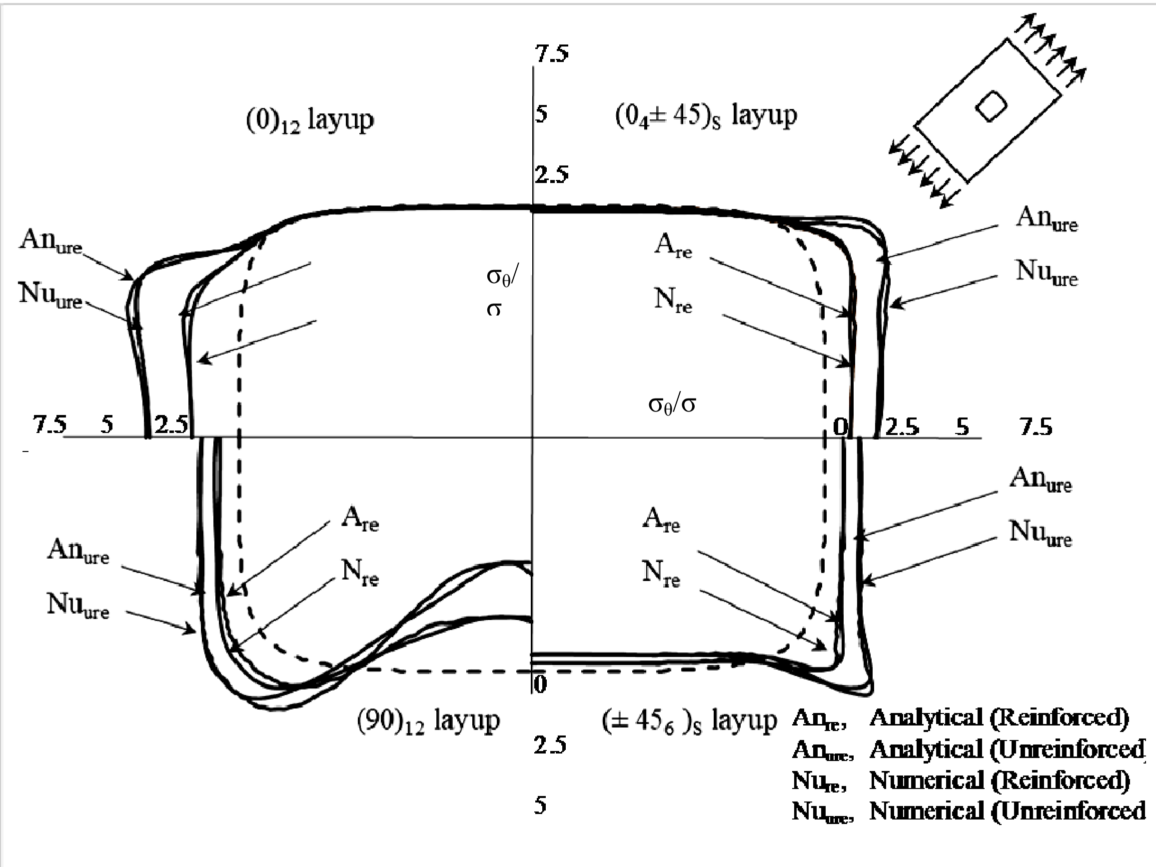

Fig.5. Stress distribution along of the hole edge in $(0)_{12}$, $(0_4 \pm 45)_S$, $(\pm 45_6)_S$ and $(90)_{12}$ laminate sequence for an unreinforced and reinforced hole.

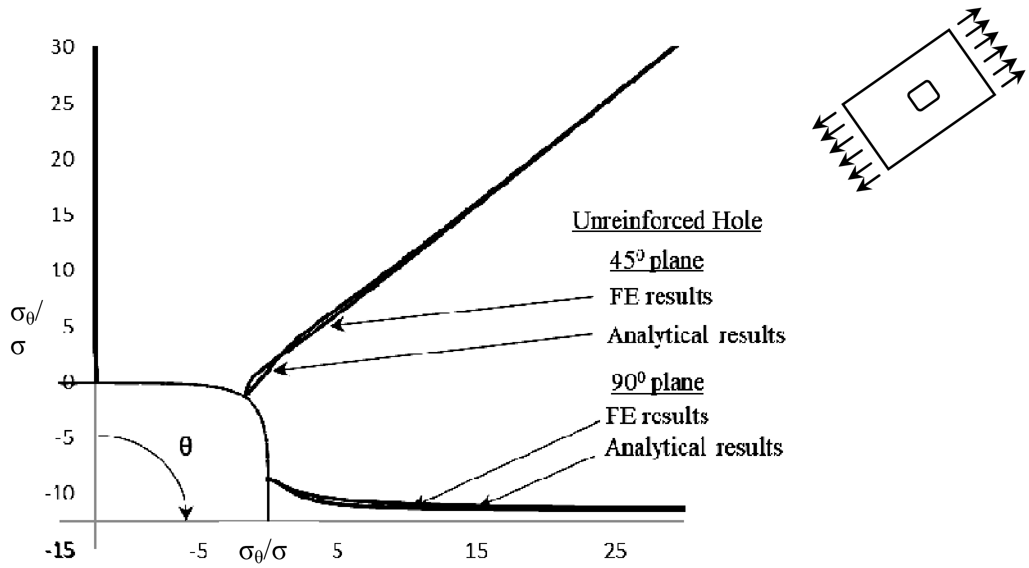

Fig.6. Full field stress distribution in $(0)_{12}$ laminate sequence.

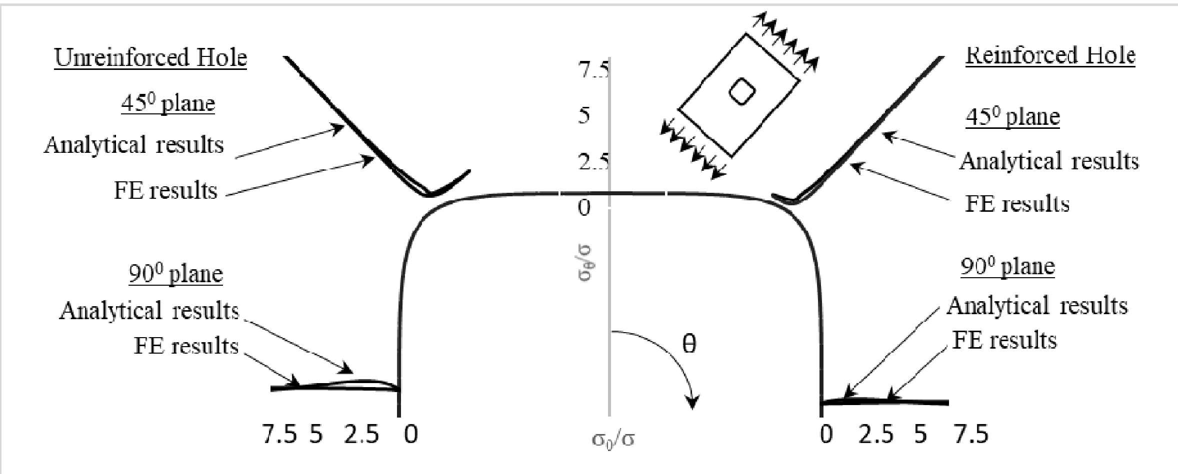

Fig.7. Stress distribution ahead of the hole edge in $(\pm 45_6)_S$ laminate sequence for a unreinforced and reinforced hole.

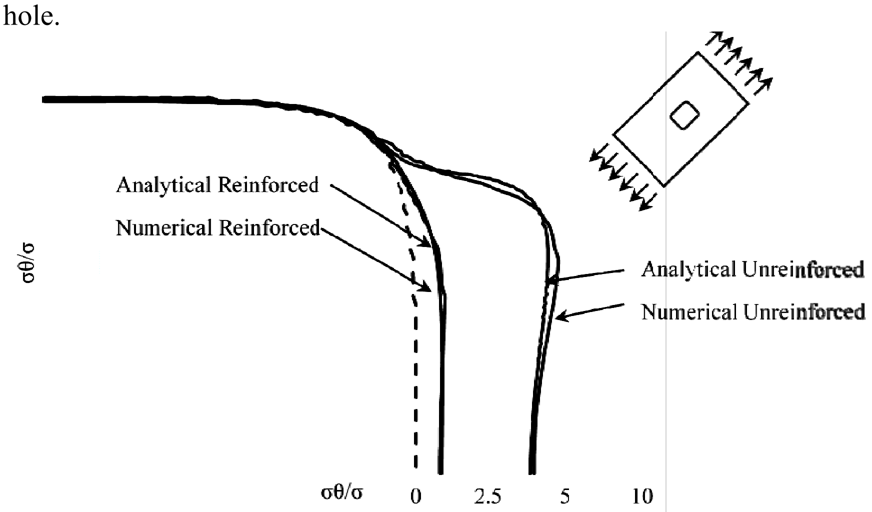

Fig.8. Stress distribution along of the hole edge in $(0)_{12}$ laminate sequence for a reinforced hole for a stress ratio of SCF.

3.1. Unreinforced hole square hole

Figure 3 shows a very good agreement of the present analytical Eq.(2.12) for the unreinforced square hole with Lekhnitskii's solution. A comparison of stress distribution ahead of the hole with the finite element analysis provided in Fig.6 and shows the efficacy of the present solution. It is concluded that present analytical equation is validated and can be considered for reinforced holes.

3.2. Reinforced hole

A comparison of the present analytical result with the finite element analysis given in Fig.4 shows convergence on peak stress value at the hole edge for a reinforcement area of *20a* x *20a* (Fig.1). Initially, for a target value of *50%* reduction in peak stress on square hole boundary which corresponds to a stress ratio given in Eq.(2.13), it is obvious that a total thickness after reinforcement should increase by two times virgin thickness. A comparison with the finite element analysis shows a good agreement for reinforced and unreinforced square holes in Fig.5 for the type of laminates considered. A comparison of the tangential stress distribution obtained from the analytical model and finite element analysis for layup sequence $(\pm 45_6)_S$ along different orientations is depicted in Fig.7 and is in good agreement with each other.

3.3. Nonsingular solution for reinforced holes

It may be noted from Fig.3 that the stress concentration factor for a square hole in a unidirectional laminate in an infinite plate under axial load is 4.9. This singularity 4.9 can be brought down to unity if the thickness of the laminate around the hole is increased by 4.9 times the virgin thickness. For such a case, the present solution for the reinforced hole gives nonsingular solution (Fig.8) as expected. A good agreement with numerical result can also be seen.

It is well known that the shell solution is the sum of plate solution and curvature effect due to the presence of a hole as obtained by Kumar *et al*. [6]. However, once a hole is reinforced, then the plate solution will be close to that of shell. This is due to the reduction in the influence of curvature effect in the proximity of the hole. Hence one may conjecture that the solution for an orthotropic shell with a reinforced noncircular hole for a given loading becomes that of plate solution with an unreinforced hole!!

4. Conclusion

The whole field tangential stress distribution in an orthotropic plate with a reinforced non circular hole has been analytically obtained for uniaxial tension case following a new methodology. The concept of expressing the noncircular hole solution for an orthotropic plate as a sum of the circular hole solution and additional terms to represent non circular holes that is governed by ε with isotropic and orthotropic material constants has been well established. For the highly orthotropic unidirectional laminate, the finite element analysis results for stress distribution around and ahead of a square hole ($\varepsilon = -1/9$) show a very good agreement with the present analytical solution. Similar conclusions have been drawn for the case of $(\pm 45)\ s$ laminate where the peak stress is close to rounded corners. It has been shown that the analytical solution is useful to overcome stress singularity with the presence of the hole by a reinforcement based on the stress ratio.

Appendix A

The contour of the square hole is described by [1] as

$$x = a\left(\cos\theta + \varepsilon\cos 3\theta\right),$$

$$y = a\left(\sin\theta - \varepsilon \sin 3\theta\right).$$

When ε is positive, the apexes of the square are located on axes *x* and *y* and in the case of negative ε, the sides are parallel to coordinate axes.

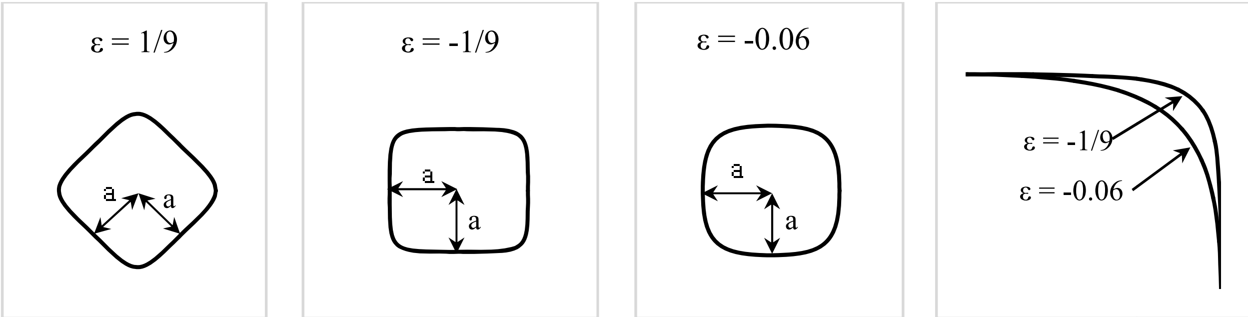

For ε = *0*, the hole will be of circular shape.

Appendix B

$$\mathrm{k} = -\mu_1\mu_2 = \sqrt{\frac{E_1}{E_2}},$$

$$n = -i\left(\mu_1 + \mu_2\right),$$

$$A = c\cos\theta - \varepsilon N \cos N\theta,$$

$$B = \sin\theta + \varepsilon N \sin N\theta,$$

$$C^2 = A^2 + B^2,$$

$$L = \left(B^2 - \mu_1^2 A^2\right)\left(B^2 - \mu_2^2 A^2\right),$$

$$D^4 = -Ak^4 + A^2B^2\left(1 - 2k - k^2\right) + B^4\left(2 + k - n^2\right),$$

$$E^4 = A^4\left(2k^2 - n^2 + k\right) + A^2B^2\left(k^2 - 2k - 1\right) - B^4 k,$$

$$g = \frac{8(1-k)}{(1+k+n)^2},$$

$$h = \frac{2}{(1+k+n)^2}\left[(1-n)^2 + k(k+2n-6)\right],$$

$$d = \frac{4}{1+k+n},$$

$$l = \frac{2}{1+k+n}(1-k-n),$$

$$r = \frac{8}{(1+k+n)^3}\left[10k - 3\left(1+k^2\right) + n(1+k)\right],$$

$$s = \frac{2}{(1+k+n)^3}\left[k^3 + 3k^2(n-11) + k\left(3n^2 - 22n + 27\right) + (n-1)^2(n-3)\right].$$

Appendix C

$$\frac{\sum_{i=0}^{\infty} x_i \varepsilon^i}{\sum_{i=0}^{\infty} X_i \varepsilon^i} = \sum_{i=0}^{\infty} c_i \varepsilon^i \tag{A.1}$$

By cross multiplying terms in the above equation

$$\sum_{i=0}^{\infty} x_i \varepsilon^i = \left(\sum_{i=0}^{\infty} c_i \varepsilon^i\right) \times \left(\sum_{i=0}^{\infty} X_i \varepsilon^i\right). \tag{A.2}$$

The above equation can be expressed as

$$\sum_{i=0}^{\infty} x_i \varepsilon^i = \left(\sum_{j=0}^{\infty} c_j \varepsilon^j\right) \times \left(\sum_{k=0}^{\infty} X_k \varepsilon^k\right), \tag{A.3}$$

$$\sum_{i=0}^{\infty} x_i \varepsilon^i = \sum_{j=0}^{\infty}\sum_{k=0}^{\infty} c_j X_k \varepsilon^{j+k}. \tag{A.4}$$

Substituting $j + k = i$

$$\sum_{i=0}^{\infty} x_i \varepsilon^i = \sum_{i=0}^{\infty}\sum_{j=0}^{i} c_j X_{i-j} \varepsilon^i \ , \tag{A.5}$$

$$\sum_{i=0}^{\infty} x_i \varepsilon^i = \sum_{i=0}^{\infty} \varepsilon^i \sum_{j=0}^{n} c_j X_{i-j} \ . \tag{A.6}$$

Equating coefficients of ε^i

$$x_i = \sum_{j=0}^{i} c_j X_{i-j} \ . \tag{A.7}$$

For $i > 0$,

$$x_i = c_i X_0 + \sum_{j=0}^{i-1} c_j X_{i-j} \ . \tag{A.8}$$

Further simplification gives

$$c_i = \frac{x_i - \sum_{j=0}^{i-1} c_j X_{i-j}}{X_o} \ . \tag{A.9}$$

Using the above expression in an iterative manner all values of c_i can be found out.

Appendix D

Elaborating Eq.(A.9), the values of c_i can be determined from the following set of equations.

$$c_1 = n_1/N_0 = (x_1 - N_1 n_0/N_0)/N_0,$$

$$c_2 = n_2/N_0 = (x_2 - (N_1 n_1/N_0 + N_2 n_0/N_0))/N_0.$$

Similarly, values of c_i up to $i = 20$ can be found out.

$$\begin{aligned} c_{20} = n_{20}/N_0 = (x_{20} - (&N_1 n_{19}/N_0 + N_2 n_{18}/N_0 + N_3 n_{17}/N_0 + N_4 n_{16}/N_0 + N_5 n_{15}/N_0 + \\ &+N_6 n_{14}/N_0 + N_7 n_{13}/N_0 + N_8 n_{12}/N_0 + N_9 n_{11}/N_0 + N_{10} n_{10}/N_0 + N_{11} n_9/N_0 + \\ &+N_{12} n_8/N_0 + N_{13} n_7/N_0 + N_{14} n_6/N_0 + N_{15} n_5/N_0 + N_{16} n_4/N_0 + N_{17} n_3/N_0 + \\ &+N_{18} n_2/N_0 + N_{19} n_1/N_0 + N_{20} n_0/N_0))/N_0. \end{aligned}$$

c_i obtained from the above expressions can be written in the form of n_i/N_0, where n_i and N_0 are cosine series as illustrated below.

$$\frac{n_i}{N_0}=\frac{\begin{pmatrix} n_{i0}+n_{i2}\cos 2\theta+n_{i4}\cos 4\theta+n_{i6}\cos 6\theta+n_{i8}\cos 8\theta+n_{i10}\cos 10\theta \\ +n_{i12}\cos 12\theta+n_{i14}\cos 14\theta+n_{i16}\cos 16\theta+n_{i18}\cos 18\theta \end{pmatrix}}{\begin{pmatrix} N_{00}+N_{02}\cos 2\theta+N_{04}\cos 4\theta+N_{06}\cos 6\theta+N_{08}\cos 8\theta+N_{010}\cos 10\theta \\ +N_{012}\cos 12\theta+N_{014}\cos 14\theta+N_{016}\cos 16\theta+N_{018}\cos 18\theta \end{pmatrix}}\ . \tag{A.10}$$

Using a standard technique illustrated by Krylov [7], the above expression can be expressed in the Fourier series as

$$\frac{S_0}{2}+\sum_{j=1}^{\infty} S_{2j}\cos 2j\theta\,. \tag{A.11}$$

Using the standard technique for determining the Fourier coefficients of a function in the above form, the coefficients S_{2j} can be found out using the following set of equations

$$N_{00}\,S_0+N_{02}\,S_2+N_{04}\,S_4+N_{06}\,S_6+N_{08}\,S_8+N_{010}\,S_{10}+N_{012}\,S_{12}+N_{014}\,S_{14}+N_{016}\,S_{16}+N_{018}\,S_{18} = n_{i0},$$

$$N_{02}\,S_0+(2\,N_{00}+N_{04})\,S_2+(N_{02}+N_{06})\,S_4+(N_{04}+N_{08})\,S_6+(N_{06}+N_{010})\,S_8+(N_{08}+N_{012})\,S_{10}+(N_{010}+N_{014})\,S_{12}+(N_{012}+N_{016})\,S_{14}+(N_{014}+N_{018})\,S_{16}+N_{016}\,S_{18}+N_{018}\,S_{20} = n_{i2}.$$

A similar set of equations can be written for j up to 8. For $j \geq 9$, a recursive relation of the following form can be used.

$$N_{018}\,S_{2j-18}+N_{016}\,S_{2j-16}+N_{014}\,S_{2j-14}+N_{012}\,S_{2j-12}+N_{010}\,S_{2j-10}+N_{08}\,S_{2j-8}+N_{06}\,S_{2j-6}+N_{04}\,S_{2j-4}+N_{02}\,S_{2j-2}+2N_{00}\,S_{2j}+N_{02}\,S_{2j+2}+N_{04}\,S_{2j+4}+N_{06}\,S_{2j+6}+N_{08}\,S_{2j+8}+N_{010}\,S_{2j+10}+N_{012}\,S_{2j+12}+N_{014}\,S_{2j+14}+N_{016}\,S_{2j+16}+N_{018}\,S_{2j+18} = n_{i2j}.$$

Values of S_{2j} can be found out by solving the above set of equations.

The same assumption of higher order terms in ρ used by Kumar *et al.*[5] in the case of a circular hole is used during the derivation of expression for full field stress distribution in an isotropic plate with a square hole.

$$f_{2j}(\rho)=-\frac{S_{2j}}{2}\left[\frac{4j-3}{\rho^{4j-2}}-\frac{4j-1}{\rho^{4j}}\right]. \tag{A.12}$$

In the case of a circular hole C_0 and C_2 are constants irrespective of the values n and k, and correspond to the value of isotropic case. But in the case of a square hole, S_0 and S_2 are not constants and hence they should be considered separately. A new assumption for higher power of ρ must be used corresponding to $j = 0$ and $j = 1$ as given below

$$\frac{S_{2j}}{4j-2}\left(\frac{4j+1}{\rho^{4j+2}}-\frac{4j+3}{\rho^{4j+4}}\right)\cos 2j\theta \tag{A.13}$$

and for values of $j > 2$ higher powers of ρ as given in Eq.(A.12) can be used.

Nomenclature

a − hole radius
E_L − Young's modulus along lateral direction
E_T − Young's modulus along transverse direction
G_{LT} − modulus of rigidity
SCF − stress concentration factor
Si − isotropic coefficients for square hole
Ss − orthotropic coefficients for square hole
t − virgin shell thickness
t_r − reinforcement thickness
u − displacement along x axis
v − displacement along y axis
ν_{LT} − Poisson's ratio
ε − hole shape parameter
σ_θ − tangential stress distribution
σ_θ /σ − distribution of tangential stress concentration factor
ρ − ratio of distance of point on the surface from centre of hole, to the width or radius of hole along x-axis or y-axis
θ − angle measured from loading direction

References

[1] Lekhnitskii S.G. (1947): *Anisotropic Plates.*− Gordon and Breach Science Publishers.

[2] Rajaiah K. and Naik N. (1982): *An analytical approach for the optimization of hole shapes in CFRP orthotropic composite plates*. − J. Aeronaut. Soc. India, pp.115-120.

[3] Whitney J. and Nuismer R. (1974): *Stress fracture criteria for laminated composites containing stress concentrations*. − J. Compos. Mater., pp.253-265.

[4] Konish H.J. and Whitney J.M. (1975): *Approximate stress in an orthotropic plate containing a circular hole*. − Journal of Composite Materials, pp.157-166.

[5] Kumar R.R., Rao G.V. and Mathew K.J. (1999): *A new solution for prediction of strength for highly orthotropic laminate with a hole*. − Journal of Aeronautical Society of India, pp.28-34.

[6] Kumar R.R., Jose S. and Rao G.V. (2001):*Analytical solution for W-N criteria for the prediction of notched strength of an orthotropic shell*. − Transactions of ASME, pp.344-346.

[7] Krylov V. (1969):*Handbook of Numerical Harmonic Analysis.* − Jerusalem: Israel Program for Scientific Tranlations.

[8] Mohan P. and Kumar R. (2017): *Analytical Prediction of Full Field Tangential Stress Distribution in Orthotropic Shell with Reinforced hole.*− Rome: ICCE 25.

Received: March 15, 2019

Revised: November 2, 2019